

# Exact method for locating potential resonances and Regge trajectories

S. A. Sofianos and S. A. Rakityansky\*

*Physics Department, University of South Africa, P.O.Box 392, Pretoria 0001, South Africa*  
(August 14, 2018)

## Abstract

We propose an exact method for locating the zeros of the Jost function for analytic potentials in the complex momentum–plane. We further extend the method to the complex angular–momentum plane to provide the Regge trajectories. It is shown, by using several examples, that highly accurate results for extremely wide as well as for extremely narrow resonances with or without the presence of the Coulomb interaction can be obtained.

PACS numbers: 03.65.Nk, 03.65.Ge, 21.45.+v

## I. INTRODUCTION

Much effort has been devoted in the past to develop methods to calculate the energies and widths of resonances in the potential scattering theory. A comprehensive survey of this subject can be found in Ref. [1]. These methods can be divided into two categories. The first one is based on methods traditionally employed for real energies where one can locate the position of relatively narrow resonances with a sufficiently high accuracy, but has many difficulties in determining their widths and usually fails for broad resonances. In the second one the calculations are performed at complex energies, and therefore the widths and resonant energies are obtained simultaneously.

The complex methods have the advantage that the calculations are based on a rigorous definition of resonances, namely, as singularities of the  $S$ –matrix. Thus, in addition to the information about the resonances themselves, they provide us with information about the analytic properties of the  $S$ –matrix and the off–shell properties of the underlying interaction. However, the existing complex–energy methods are much more complicated than those of the first group and require sophisticated mathematical and computational methods to handle them.

Usually, the complex methods are referred to as the “direct calculation approaches”, but very often with the quotation marks [2] because most of them are based on an expansion

---

\*Permanent address: Joint Institute for Nuclear Research, Dubna, 141980, Russia

of the resonant wave function in terms of square integrable functions and the subsequent determination of the expansion coefficients either by a diagonalization of the non-Hermitian Hamiltonian or by a variational procedure.

The method we present here formally belongs to the second group i.e., to the complex-energy methods. It is based on exact differential equations for functions closely related to the Jost solutions and which coincide with the Jost functions at large distances [3–5]. Unlike the existing methods, it is simple in applications and although it exploits the idea of the complex rotation of the coordinates, it is different from the traditionally used complex dilation methods in that it does not employ expansion or variational procedures. Instead, the Jost function at a complex energy is obtained directly from exact equations equivalent to the Schrödinger equation.

To demonstrate the effectiveness and accuracy of our approach, we performed calculations using potentials previously employed by other authors [6–9]. We not only located the resonances cited by them but also find sequences of Jost function zeros corresponding to broad and extremely narrow resonances which were not considered or missed in the aforementioned references.

In addition to the location of zeros in the complex  $k$ -plane, the present method enables us to locate the zeros of Jost functions in the complex angular momentum plane. We demonstrated this by locating the zeros, known as Regge poles, representing resonances in the complex  $\ell$ -plane.

The paper is organized as follows. In Sec. II our formalism is presented, while Sec. III is devoted to the boundary conditions. In Sec. IV the method is applied to several examples and the results obtained are discussed and compared with those obtained by other methods.

## II. BASIC EQUATIONS

Consider the one-channel problem of two, generally charged, particles. Apart from the Coulomb force, we assume that these particles interact via a central potential  $V(r)$  having the properties

$$\lim_{r \rightarrow 0} r^2 V(r) = 0 \tag{1}$$

and

$$\lim_{r \rightarrow \infty} r V(r) = 0. \tag{2}$$

The radial Schrödinger equation reads ( $\hbar = 1$ )

$$\left[ \partial_r + 2mk^2 - \ell(\ell + 1)/r^2 - 2\eta k/r \right] \Phi_\ell(k, r) = V(r) \Phi_\ell(k, r). \tag{3}$$

The regular solutions  $\Phi_\ell(k, r)$ , for any complex  $k \neq 0$  and complex  $\ell$  in the half-plane  $\text{Re } \ell > -1/2$ , are defined by the boundary condition

$$\lim_{r \rightarrow 0} [\Phi_\ell(k, r)/F_\ell(\eta, kr)] = 1, \quad (4)$$

where  $F_\ell(\eta, kr)$  is the regular Coulomb function [10].

In contrast to  $\Phi_\ell(k, r)$ , the physical solutions (bound, scattering, and Siegert states) are defined by their behaviour at large distances. However, they all are regular at  $r = 0$  and thus proportional to  $\Phi_\ell(k, r)$ . Therefore, once the function  $\Phi_\ell(k, r)$  is determined at all complex momenta  $k$ , it represents, in a most general form, all solutions of physical interest of Eq. (3) since any physical solution at specific values of  $k$  can be obtained from it merely by multiplying  $\Phi_\ell(k, r)$  by the proper normalization constant.

At large distances  $\Phi_\ell(k, r)$  can be written as a linear combination

$$\Phi_\ell(k, r) \xrightarrow{r \rightarrow \infty} \frac{1}{2} \left[ H_\ell^{(+)}(\eta, kr) f_\ell^*(\eta, k^*) + H_\ell^{(-)}(\eta, kr) f_\ell(\eta, k) \right]. \quad (5)$$

The functions  $H_\ell^{(\pm)}(\eta, z)$  are defined in terms of the regular  $F_\ell(\eta, z)$  and irregular  $G_\ell(\eta, z)$  Coulomb functions [10,11,15],

$$H_\ell^{(\pm)}(\eta, z) \equiv F_\ell(\eta, z) \mp i G_\ell(\eta, z), \quad (6)$$

and have the asymptotic behaviour,

$$H_\ell^{(\pm)}(\eta, z) \xrightarrow{|z| \rightarrow \infty} \mp i \exp\left\{ \pm i [z - \eta \ln 2z - \ell\pi/2 + \arg\Gamma(\ell + 1 + i\eta)] \right\}. \quad (7)$$

For neutral particles or high energies where the Sommerfeld parameter  $\eta \rightarrow 0$ , the Coulomb functions reduce to the Riccati–Bessel, Riccati–Neumann, and Riccati–Hankel functions [10], i.e.,

$$\begin{aligned} F_\ell(\eta, z) &\xrightarrow{\eta \rightarrow 0} J_\ell(z), \\ G_\ell(\eta, z) &\xrightarrow{\eta \rightarrow 0} -n_\ell(z), \\ H_\ell^{(\pm)}(\eta, z) &\xrightarrow{\eta \rightarrow 0} h_\ell^{(\pm)}(z). \end{aligned}$$

The momentum–dependent coefficients in the above linear combination, Eq. (5), are the Jost functions which are analytical for all complex  $k$  of physical interest and for  $\text{Re } \ell > -1/2$ . The last restriction on  $\ell$  stems from the fact that at  $\text{Re } \ell = -1/2$  the role of  $F_\ell(\eta, z)$  and  $G_\ell(\eta, z)$ , of being regular and irregular at the origin, is interchanged [11].

For integer (physical)  $\ell$  the Jost function has zeros at a discrete sequence of points  $k_{0i}$ ,  $i = 1, 2, 3, \dots$ , situated either on the imaginary axis of the  $k$ –plane or under the real axis. At these points only the first term in the asymptotic form (5) survives, corresponding to either a bound ( $\text{Im } k > 0$ ) or a Siegert ( $\text{Im } k < 0$ ) state behaviour for large  $r$ .

On the other hand, for real values of  $k^2$  (physical energies), the function  $f_\ell(\eta, k)$  can have zeros at complex  $\ell$  which move, with increasing  $k^2$ , along the so–called Regge trajectories

which define families of bound and resonant states [11]. Therefore, when the Jost function is known at all complex values of  $k$  and at all permissible values of  $\ell$ , it contains all information and characteristics of the spectrum of the underlying physical system.

In Ref. [5] we proposed a method for a direct calculation of the Jost function for any complex momentum of physical interest. In this approach we use a combination of the variable–constant [12] and the complex coordinate–rotation [13] methods to solve the Schrödinger equation (3) in an efficient and accurate way without resorting to any approximation, expansion, or to variational (stabilization) procedures. For this, we perform a complex rotation of the coordinate  $r$

$$r = x \exp(i\theta), \quad x \geq 0, \quad \theta \in [0, \theta_{max}], \quad \theta_{max} < \pi/2 \quad (8)$$

in the Schrödinger equation (3) and look for a solution in the form

$$\Phi_\ell(k, r) = \frac{1}{2} \left[ H_\ell^{(+)}(\eta, kr) \mathcal{F}_\ell^{(+)}(\eta, k, x, \theta) + H_\ell^{(-)}(\eta, kr) \mathcal{F}_\ell^{(-)}(\eta, k, x, \theta) \right], \quad (9)$$

where  $\mathcal{F}_\ell^{(\pm)}(\eta, k, x, \theta)$  are new unknown functions (variable constants) which at large  $x$  become, according to Eq. (5), true constants. In this way the initial value problem, defined by Eqs. (3) and (4), reduces to the following first–order coupled differential equations

$$\begin{aligned} \partial_x \mathcal{F}_\ell^{(+)}(\eta, k, x, \theta) = & \frac{e^{i\theta}}{2ik} H_\ell^{(-)}(\eta, kr) V(r) \\ & \times \left[ H_\ell^{(+)}(\eta, kr) \mathcal{F}_\ell^{(+)}(\eta, k, x, \theta) + H_\ell^{(-)}(\eta, kr) \mathcal{F}_\ell^{(-)}(\eta, k, x, \theta) \right], \end{aligned} \quad (10)$$

$$\begin{aligned} \partial_x \mathcal{F}_\ell^{(-)}(\eta, k, x, \theta) = & -\frac{e^{i\theta}}{2ik} H_\ell^{(+)}(\eta, kr) V(r) \\ & \times \left[ H_\ell^{(+)}(\eta, kr) \mathcal{F}_\ell^{(+)}(\eta, k, x, \theta) + H_\ell^{(-)}(\eta, kr) \mathcal{F}_\ell^{(-)}(\eta, k, x, \theta) \right], \end{aligned} \quad (11)$$

with the simple boundary conditions

$$\mathcal{F}_\ell^{(+)}(\eta, k, 0, \theta) = \mathcal{F}_\ell^{(-)}(\eta, k, 0, \theta) = 1, \quad (12)$$

which follow immediately from Eqs. (4), (6), and (9).

In Ref. [5] it was proved that if the potential obeys the conditions (1) and (2), with complex  $r$  defined by (8), then for all complex  $k$  situated above the dividing line  $|k| \exp(-i\theta)$  and for  $x \rightarrow \infty$ , the function  $\mathcal{F}_\ell^{(-)}(\eta, k, x, \theta)$  has a  $\theta$ –independent limit which coincides with the Jost function, i.e.,

$$\lim_{x \rightarrow \infty} \mathcal{F}_\ell^{(-)}(\eta, k, x, \theta) = f_\ell(\eta, k), \quad (13)$$

while the function  $\mathcal{F}_\ell^{(+)}(\eta, k, x, \theta)$  converges to  $f_\ell^*(\eta, k^*)$  at all spectral points  $k_{0i}$ ,  $i = 1, 2, 3, \dots$ , for which  $f_\ell(\eta, k_{0i}) = 0$ .

The proof was based on the asymptotic behaviour of the functions  $H_\ell^{(\pm)}(\eta, kr)$  at large  $r$ , and can be generalized to include the complex angular momentum  $\ell$  as well. This generalization is straightforward since the angular momentum appears only in the phase factor of the asymptotic form, Eq. (7), and therefore for a complex  $\ell$  the functions  $\mathcal{F}_\ell^{(\pm)}(\eta, k, x, \theta)$  at large  $x$  have the same behaviour and the asymptotic relation (13) is also valid.

Thus, the procedure of calculating the Jost function is very simple since for any fixed pair of  $k$  and  $\ell$  we only need to solve the system of first-order differential equations (10) and (11) from  $x = 0$  to some  $x_{max}$  where  $\mathcal{F}_\ell^{(-)}(\eta, k, x, \theta)$  attains a constant value (usually,  $x_{max}$  is the range of the potential  $V$ ). According to Eq. (13), this constant is just the Jost function  $f_\ell(\eta, k)$  we are looking for. Simultaneously, as a bonus, we obtain the exact wave function in the form of Eq. (9) having the correct asymptotic behaviour. Depending on the choice of the momentum  $k$ , it can be a bound, scattering, or a Siegert state wave function (rotated when  $\theta > 0$ ).

The resonances in a specific region of complex  $k$  can be easily located by taking the rotation angle  $\theta$  large enough to cover this region and then search for zeros of the Jost function. The zeros in the complex  $\ell$ -plane can be similarly located with  $\theta = 0$ .

We emphasize that this method is exact. Although we employ the complex rotation, we do not need any stabilization procedure. This has been demonstrated in Ref. [5] where we employed an analytically solvable model and showed that Eqs. (10) and (11) give at least 5-digit accuracy for the Jost function in a wide area of complex  $k$  despite the fact that the simplest Runge-Kutta method of integration was used.

### III. BOUNDARY CONDITIONS

#### A. Short distances

Formally, we have to start the integration of Eqs. (10) and (11) from  $x = 0$ . However, for  $\ell \neq 0$  the functions  $H_\ell^{(\pm)}(\eta, kr)$  are irregular, i.e., at the origin they behave as [14]

$$H_\ell^{(\pm)}(\eta, kr) \xrightarrow{r \rightarrow 0} \frac{\mp i}{2^\ell(2\ell + 1)C_\ell(\eta)} \left(\frac{kr}{2}\right)^{-\ell} + \begin{cases} \mathcal{O}(\eta kr \ln kr), & \text{for } \ell = 0 \\ \mathcal{O}(\eta(kr)^{1-\ell}), & \text{for } \ell \neq 0, \end{cases}$$

where

$$C_\ell(\eta) = \frac{2^\ell \exp(-\pi\eta/2)}{\Gamma(2\ell + 2)} [\Gamma(\ell + 1 + i\eta)\Gamma(\ell + 1 - i\eta)]^{1/2} .$$

In Ref. [5] it was shown that the corresponding singularities at  $x = 0$  in the above differential equations (10) and (11) are integrable when the condition (1) is fulfilled. Thus, there is no problem from a formal point of view. However, in practical calculations we cannot start from  $x = 0$  and therefore we have to shift the initial point to some small value  $x_{min}$ . Thus, to implement the boundary conditions, we need to know  $\mathcal{F}_\ell^{(\pm)}(\eta, k, x_{min}, \theta)$ .

There are several ways to circumvent this problem. One of them consists in transforming the differential equations, Eqs. (10) and (11), into an equivalent pair of integral Volterra-type equations, viz.,

$$\mathcal{F}_\ell^{(\pm)}(\eta, k, x, \theta) = 1 \pm \frac{e^{i\theta}}{ik} \int_0^x H_\ell^{(\mp)}(\eta, kx'e^{i\theta})V(x'e^{i\theta})\Phi_\ell(k, x'e^{i\theta})dx' , \quad (14)$$

where  $\Phi_\ell(k, r)$  is defined by Eq. (9). We can solve these integral equations in the interval  $[0, x_{min}]$  iteratively as follows:

$$\begin{aligned} \mathcal{F}_\ell^{(\pm)(0)}(\eta, k, x_{min}, \theta) &= 1 , \\ \mathcal{F}_\ell^{(\pm)(1)}(\eta, k, x_{min}, \theta) &= 1 \pm \frac{e^{i\theta}}{ik} \int_0^{x_{min}} H_\ell^{(\mp)}(\eta, kxe^{i\theta})V(xe^{i\theta})F_\ell(\eta, kxe^{i\theta})dx , \\ &\vdots \\ \mathcal{F}_\ell^{(\pm)(N)}(\eta, k, x_{min}, \theta) &= 1 \pm \frac{e^{i\theta}}{2ik} \int_0^{x_{min}} H_\ell^{(\mp)}(\eta, kxe^{i\theta})V(xe^{i\theta}) \\ &\times \left[ H_\ell^{(+)}(\eta, kxe^{i\theta})\mathcal{F}_\ell^{(+)(N-1)}(\eta, k, x, \theta) + H_\ell^{(-)}(\eta, kxe^{i\theta})\mathcal{F}_\ell^{(-)(N-1)}(\eta, k, x, \theta) \right] , \end{aligned} \quad (15)$$

and then integrate the differential equations starting from the value of  $\mathcal{F}_\ell^{(\pm)(N)}(\eta, k, x_{min}, \theta)$ .

For small values of  $x_{min}$  the above iteration procedure converges very fast. Moreover, in implementing the method we found that if  $\text{Re } \ell$  is small ( $\sim 1$ ), then a surprisingly high accuracy (better than 7-digits) can be achieved even with the lowest order iteration, Eq. (15). For higher values of  $\text{Re } \ell$ , however, the use of these simple boundary conditions could result in numerical instabilities. This is due to the ansatz (9) which is suitable for large distances, but is not good in the vicinity of  $r = 0$ . Indeed, near this point the function  $\Phi_\ell(k, r)$ , by its definition, is regular and therefore the singularities of  $H_\ell^{(+)}(\eta, kr)$  and  $H_\ell^{(-)}(\eta, kr)$  are cancelled. This is secured by the boundary conditions (12). In numerical calculations, however, the cancellation of singularities is always a precarious procedure and a source of possible numerical errors. These errors increase with increasing  $\text{Re } \ell$  since in this case  $H_\ell^{(\pm)}(\eta, kr)$  is more singular. Therefore, the greater  $\text{Re } \ell$  is the further the point  $x_{min}$  must be shifted from the origin in order to avoid cancellation errors. This shift in turn, requires more iterations of Eq. (14) to obtain the boundary values  $\mathcal{F}_\ell^{(\pm)}(\eta, k, x_{min}, \theta)$  to a required accuracy.

Another way to handle the boundary condition problem is to replace at short distances the ansatz (9) by a more suitable one. Indeed, this ansatz was motivated by the variable constant method [12], i.e. we looked for a solution of Eq. (3) in the form of a linear combination of its two independent solutions  $H_\ell^{(+)}$  and  $H_\ell^{(-)}$  corresponding to  $V(r) \equiv 0$ . When the potential is taken into account, the coefficients of this combination are  $r$ -dependent and obey the Eqs. (10) and (11). Thus, instead of  $H_\ell^{(\pm)}(\eta, kr)$  we can choose another pair of linearly independent solutions, namely,  $F_\ell(\eta, kr)$  and  $G_\ell(\eta, kr)$ , and the new ansatz reads

$$\Phi_\ell(k, r) = F_\ell(\eta, kr)A_\ell(\eta, k, x, \theta) + G_\ell(\eta, kr)B_\ell(\eta, k, x, \theta) . \quad (16)$$

Since (9) and (16) are merely different representations of the same function, we have

$$\mathcal{F}_\ell^{(\pm)}(\eta, k, x, \theta) \equiv A_\ell(\eta, k, x, \theta) \pm iB_\ell(\eta, k, x, \theta), \quad (17)$$

and the equations for the functions  $A_\ell(\eta, k, x, \theta)$  and  $B_\ell(\eta, k, x, \theta)$  are

$$\begin{aligned} \partial_x A_\ell(\eta, k, x, \theta) = & \\ & \frac{e^{i\theta}}{k} G_\ell(\eta, kr) V(r) [F_\ell(\eta, kr) A_\ell(\eta, k, x, \theta) + G_\ell(\eta, kr) B_\ell(\eta, k, x, \theta)], \end{aligned} \quad (18)$$

$$\begin{aligned} \partial_x B_\ell(\eta, k, x, \theta) = & \\ & - \frac{e^{i\theta}}{k} F_\ell(\eta, kr) V(r) [F_\ell(\eta, kr) A_\ell(\eta, k, x, \theta) + G_\ell(\eta, kr) B_\ell(\eta, k, x, \theta)]. \end{aligned} \quad (19)$$

The corresponding boundary conditions,

$$A_\ell(\eta, k, 0, \theta) = 1, \quad B_\ell(\eta, k, 0, \theta) = 0, \quad (20)$$

follow immediately from (12) and (17).

In other words, we have two equivalent pairs of equations, Eqs. (10) and (11) and (18) and (19), defining the same function  $\Phi_\ell(k, r)$  in its two different representations (9) and (16). Computationally it is easier to start the integration of equations (18) and (19) at  $x_{min}$  and continue it up to some intermediate point  $x_{int}$  (not necessary small), and then to integrate the equations (10) and (11) from  $x_{int}$  to  $x_{max}$  where  $\mathcal{F}_\ell^{(-)}(\eta, k, x_{max}, \theta)$  coincides with the Jost function.

Similarly to equations (10) and (11) the differential equations for  $A_\ell(\eta, k, x, \theta)$  and  $B_\ell(\eta, k, x, \theta)$  can be transformed into integral Volterra-type equations,

$$A_\ell(\eta, k, x, \theta) = 1 + \frac{e^{i\theta}}{k} \int_0^x G_\ell(\eta, kx' e^{i\theta}) V(x' e^{i\theta}) \Phi_\ell(k, x' e^{i\theta}) dx', \quad (21)$$

$$B_\ell(\eta, k, x, \theta) = - \frac{e^{i\theta}}{k} \int_0^x F_\ell(\eta, kx' e^{i\theta}) V(x' e^{i\theta}) \Phi_\ell(k, x' e^{i\theta}) dx', \quad (22)$$

where  $\Phi_\ell(k, r)$  is defined by Eq. (16). Iterations of these integral equations can also be used to obtain corrections, if necessary, to the simplest form of the boundary conditions, namely,

$$A_\ell(\eta, k, x_{min}, \theta) = 1, \quad B_\ell(\eta, k, x_{min}, \theta) = 0. \quad (23)$$

## B. Large distances

The behaviour of  $\Phi_\ell(k, r)$  at large distance, is determined by the functions  $H_\ell^{(\pm)}(\eta, kr)$ . Therefore, the correct asymptotic form is automatically secured.

Indeed, suppose we have found on the positive imaginary axis of the  $k$ -plane a value  $k_0$  for which  $\mathcal{F}_\ell^{(-)}(\eta, k_0, x_{max}, 0) = 0$  (when  $\text{Im } k \geq 0$  we can always put  $\theta = 0$ ), i.e., we located a zero of the Jost function corresponding to a bound state. The physical bound state wave function is then given by,

$$\varphi_\ell^{bound}(k_0, r) = \mathcal{N} \Phi_\ell(k_0, r),$$

and differs from  $\Phi_\ell(k_0, r)$  only by a normalization factor  $\mathcal{N}$  which can, in principle, be found along with  $\Phi_\ell(k_0, r)$  in terms of the Jost function and its derivative [15,16], or simply from the normalization integral. At large  $r$  only the first term of Eq. (9) survives, i.e.,

$$\Phi_\ell(k_0, r) \xrightarrow{|r| \rightarrow \infty} \frac{1}{2} \mathcal{F}_\ell^{(+)}(\eta, k_0, x_{max}, 0) H_\ell^{(+)}(\eta, k_0 r). \quad (24)$$

Obviously, in this expression the exponentially decaying tail of the bound state wave function is presented in an exact form.

For scattering states (real positive  $k$ ), the asymptotic form of  $\Phi_\ell(k, r)$  contains both terms of Eq. (9),

$$\Phi_\ell(k, r) \xrightarrow{|r| \rightarrow \infty} \frac{1}{2} \left[ H_\ell^{(+)}(\eta, kr) \mathcal{F}_\ell^{(+)}(\eta, k, x_{max}, 0) + H_\ell^{(-)}(\eta, kr) \mathcal{F}_\ell^{(-)}(\eta, k, x_{max}, 0) \right], \quad (25)$$

where the functions  $H_\ell^{(\pm)}(\eta, kr)$  represent the incoming and outgoing spherical waves (again in the exact form). The scattering wave function,  $\varphi_{\ell, k}^{scatt}(r)$ , differs from  $\Phi_\ell(k, r)$  only by a constant factor, viz.,

$$\varphi_{\ell, k}^{scatt}(r) = \frac{1}{2\mathcal{F}_\ell^{(-)}(\eta, k, x_{max}, 0)} \left[ H_\ell^{(+)}(\eta, kr) \mathcal{F}_\ell^{(+)}(\eta, k, x, 0) + H_\ell^{(-)}(\eta, kr) \mathcal{F}_\ell^{(-)}(\eta, k, x, 0) \right], \quad (26)$$

where we assumed that the scattering states  $|\Psi_{\vec{k}}^{scatt}\rangle$  are normalized according to

$$\langle \Psi_{\vec{k}'}^{scatt} | \Psi_{\vec{k}}^{scatt} \rangle = \delta(\vec{k}' - \vec{k})$$

and expanded in partial waves as follows:

$$\langle \vec{r} | \Psi_{\vec{k}}^{scatt} \rangle = \sqrt{\frac{2}{\pi}} \frac{1}{kr} \sum_{\ell m} i^\ell \varphi_{\ell, k}^{scatt}(r) Y_{\ell m}^*(\hat{k}) Y_{\ell m}(\hat{r}).$$

For the Siegert states, corresponding to zeros of  $\mathcal{F}_\ell^{(-)}(\eta, k, x_{max}, \theta)$  in the lower half of the  $k$ -plane, we have the same kind of asymptotic behaviour as in  $\Phi_\ell(k_0, r)$  given by Eq. (24) but in this case  $\theta > 0$ , and therefore such states can be treated and normalized similarly to bound states [2].

In summary, the representation (16) secures the proper behaviour of  $\Phi_\ell(k, r)$  at short distances, while the representation (9) guarantees its correct behaviour at large  $r$ . The use of these representations enables us to achieve high accuracy in the solution of Eq. (3) at all complex values of  $k$ .

#### IV. NUMERICAL EXAMPLES

In order to demonstrate the ability and accuracy of the proposed method, we chose two simple potentials previously used in Refs. [6–9]. This choice is further motivated by the

richness of the spectra generated by these potentials and by their simple form. And, as we found, their spectra include very wide as well as extremely narrow resonances which are difficult to locate with most of the existing methods. Thus they are ideally suited as testing cases.

In atomic units [17], these potentials have the following form

$$V_1(r) = 7.5r^2 \exp(-r) + \frac{z}{r}$$

and

$$V_2(r) = 5 \exp[-0.25(r - 3.5)^2] - 8 \exp(-0.2r^2) .$$

The reader not accustomed to the atomic units, may assume that the above potentials are given in MeV and the distances in fm. In such a case  $\hbar^2/2m = 1/2$  MeV fm<sup>2</sup> while the Sommerfeld parameter is given by  $\eta = z/k$ . Then the numerical values of the resonance energies are the same and independent of the unit used (MeV or atomic units a.u.). In what follows, in order to avoid possible misunderstanding, we will use the MeV-fm units. We note that  $V_1(r)$  is a good case to test the ability of the method to deal with interactions having a Coulomb tail. Similarly to Ref. [9] we assumed that the Coulomb part is attractive with  $z = -1$ . In order to compare our results with those given in Refs. [6–8], we also performed calculations with  $z = 0$ .

To locate zeros of the Jost function in the complex  $k$ -plane as well as in the complex  $\ell$ -plane, we searched for minima of its modulus,  $|\mathcal{F}_\ell^{(-)}(\eta, k, x_{max}, \theta)|$ , considered as a function of two variables, either  $\text{Re } k$  and  $\text{Im } k$  or  $\text{Re } \ell$  and  $\text{Im } \ell$ . This is based on the so called maximum modulus principle for a complex-valued function [18]. According to this principle, when a function  $f(z)$  is holomorphic and not constant in a region  $D$  of the complex plane,  $|f(z)|$  can never attain its maximum in the interior of  $D$  but only on the boundary of  $D$ . Therefore the minima of  $|f(z)|$  must coincide with the zeros of  $f(z)$ . Indeed, assuming that  $|f(z)|$  has a minimum at  $z = z_0$  inside the area  $D$  and  $f(z_0) \neq 0$  then around the point  $z_0$  the function  $1/f(z)$  is holomorphic and has a maximum inside an area, which contradicts the maximum modulus principle. Thus, if a minimum of  $|f(z)|$  is found, it must be the zero of  $f(z)$ .

The located zeros of the Jost function in the fourth quadrant of the complex  $k$ -plane for the potential  $V_1(r)$  for the  $\ell = 0$  partial wave, and the corresponding resonance energies and widths are presented in Table I together with the results of Refs. [6–9]. Our calculations have been performed with the simplest boundary condition (23). This was sufficient to achieve an accuracy of at least 9 digits. This is checked by changing the rotation angle  $\theta$  since the Jost function must be  $\theta$ -independent. We note that only few  $S$ -wave resonances are presented although many more were located. The reason is that this potential has been used earlier by several authors (but only for the case  $\ell = 0$ ) and thus we employed it in order to compare our results with those of Refs. [6–9]. The sequence of the  $S$ -wave resonant zeros continues downwards in the complex  $k$ -plane. This behaviour can be seen in Fig. 1 where these zeros are plotted. A similar behaviour was also found for resonances of higher partial waves. In these cases, however, the first few zeros of the sequences are closer to the

real axis (which means that they have a smaller width). The same trends were found for the resonances of the potential  $V_2(r)$  which generates a richer spectrum.

Comparison with the other calculations for the potential  $V_1(r)$  shows (see Table I) that only the “direct” (dilatation) method of Ref. [6] gives an accuracy which is comparable with ours. In that reference, the 5–digit accuracy was achieved by using over 40 exponentially decreasing functions in the expansion of the rotated Siegert state. In contrast a 9–digits accuracy is achieved by our method without any exertion and, if necessary, can easily be improved. Such an improvement is of crucial importance when one deals with extremely narrow resonances. When the width of a resonance is 7 orders of magnitude less than its energy, one needs at least a 7–digit accuracy to be able to discern it.

Another extreme situation is the case of very broad resonances, i.e., when the Jost function zeros are situated far below the real axis. As can be seen in Table I, even for the first resonance ( $E_0 = 3.426390331$  MeV,  $\Gamma = 0.025548962$  MeV) only a third digit accuracy in the width has been achieved by the “real–energy methods” of Refs. [7,8] and by the “semi–complex method” of Ref. [9] while the next, moderately broad, resonance ( $E_0 = 4.834806841$  MeV,  $\Gamma = 2.235753338$  MeV), is already beyond their resolution.

The “real–energy methods” of Refs. [7,8] consider eigenenergies of a system enclosed in a box. These eigenenergies are moving together with the change of the radius of the box, generating the so–called quasi–crossings at resonance energies. The width of a resonance is determined by the breadth of the quasi–crossing. Such an approach exploits the physical idea that the resonant states, are only slightly affected by variations of the radius of the box, in contrast to the spurious states that emerge in the box. It seems, however, that this idea is not suitable for broad resonant states. Indeed, in Fig. 1 of Ref. [7] and Fig. 1 of Ref. [8], presenting the box eigenenergies, no traces of the the second quasi–crossing of the  $S$ –wave resonance at  $E = 4.834806841$  MeV or of the third at  $E = 5.277279780$  MeV can be found.

It is claimed that broad resonances are unimportant and thus the inability of a method to describe them is a minor drawback. However, in certain physical systems, broad resonances play a significant role. An example is the  $S_{11}(1535)$  resonance of the interaction of the  $\eta$ –meson with a nucleon which lies 48 MeV above the threshold while its width is 150 MeV [19]. Nevertheless it prescribes the dynamics of the  $\eta$ –meson interaction with nuclei. In particular, due to this resonance, certain  $\eta$ –nucleus systems can have quasi–bound states [20].

One of the advantages of the exact method presented in this work, is that bound, scattering, and resonant states can be treated in a uniform way regardless of their width. All spectral points can be located with the same accuracy irrespective of their location on the complex  $k$ –plane. This is exemplified by the spectral analysis of the potential  $V_2(r)$ . Sequences of the bound and resonant states generated by this potential are given in Tables II and III. The  $S$ – and  $P$ –wave sequences are also shown in Fig. 2.

The  $S$ –wave states, generated by the potential  $V_2(r)$ , were previously considered in Ref.

[7], where only the first two resonances were found. As can be seen in Table II, the spherical-box method of Ref. [7] provides the position of the first (narrow) resonance fairly well. However, the width is obtained only to two correct digits. For the second resonance, which is broader than the first one, the accuracy for the energy evaluation is down to 3 digits and for the width just to 1 digit. The other resonances of the  $S$ -wave sequence, presented in Table II, were not obtained with the box-method.

The accuracy of the present method is determined by the accuracy of solution of the differential equations. By choosing the tolerance to be small enough we can locate practically all resonances. Two remarkable examples of extremely narrow resonances, generated by the potential  $V_2(r)$ , are the one found for the  $P$ -wave at  $E_0 = 0.807634844$  MeV ( $\Gamma = 0.110 \times 10^{-6}$  MeV) and the other for the  $F$ -wave at  $E_0 = 1.009031953$  MeV ( $\Gamma = 0.46 \times 10^{-7}$  MeV) and are parts of the sequences presented in Table III. If the attraction of the potential is slightly increased, these extremely narrow resonances become bound states in the  $P$  and  $F$  partial waves.

Some of the Jost-function zeros found in the complex  $\ell$ -plane are given in Tables IV and V. The corresponding Regge trajectories are depicted in Fig. 3. Each trajectory begins from an  $S$ -wave spectral state. The first one begins from the ground state and passes via the lowest states of each partial wave. When the energy is negative, the trajectory lies on the real axis, while at positive energies it gradually goes upwards. We note that the width of a narrow resonance can, in principle, be found via  $\text{Im } \ell$  which corresponds to an integer value of  $\text{Re } \ell$ . However, the relation between  $\Gamma$  and  $\text{Im } \ell$  involves also the derivative of the trajectory [16].

The Regge trajectories, can provide us with a useful information on the spectrum of the physical system. They combine bound and resonant states in families and therefore in calculating such trajectories, we can find out at which energies and in which partial waves resonances must exist. Furthermore, the Regge trajectories give us a general insight into the spectrum of the Hamiltonian under consideration. For example, we can state that the  $F$ -wave resonance at  $E = 1.009031953$  MeV is the narrowest one for the potential  $V_2(r)$ . This follows from the fact that this resonance belongs to the lowest Regge trajectory and is the first on it.

In conclusion, the method we present in this article, enables us to locate the zeros of the Jost function in the complex  $k$ -plane and to calculate the Regge trajectories in the complex  $\ell$ -plane in a simple, efficient, and extremely accurate way. To the best of our knowledge, no other method achieved such a performance in the past. Since it is based on exact equations, the method simultaneously provide us with the corresponding wave functions of the spectral states.

As a final note we mention that the method can be easily generalized to treat the coupled channel problems having the same angular momentum. In such a case we replace the potential and the functions  $\mathcal{F}_\ell^{(\pm)}(\eta, k, x, \theta)$  by matrices and the spectrum is then defined by the zeros of the Jost-matrix determinant. Channels of different angular momenta can

also be treated in the same manner, but this requires a more elaborate treatment of the boundary conditions at  $x = 0$  since some off-diagonal elements of the matrices  $\mathcal{F}_\ell^{(\pm)}$  for different  $\ell$  may be singular at the origin. Nonlocal potentials can also be considered within the proposed approach. Work on all these generalizations is under way.

### ACKNOWLEDGMENTS

One of us (S.A.R) gratefully acknowledges financial support from the University of South Africa and the Joint Institute for Nuclear Research, Dubna.

TABLES

TABLE I. The zeros  $k_0$  of the Jost function in the complex  $k$ -plane and the energies  $E_0$  and widths  $\Gamma$  of the  $S$ -wave resonances for the potential  $V_1(r)$  with ( $z = -1$ ) and without ( $z = 0$ ) the Coulomb term.

$z$	$k_0$ ( $\text{fm}^{-1}$ )	$E_0$ (MeV)	$\Gamma$ (MeV)	Ref.
0	2.617786172 - $i$ 0.004879876	3.426390331	0.025548962	this work
		3.42639	0.025549	[6]
		3.4257	0.0256	[7]
		3.426	0.0256	[8]
		3.426	0.0258	[9]
0	3.130042444 - $i$ 0.357144253	4.834806841	2.235753338	this work
0	3.398392393 - $i$ 0.997251873	5.277279780	6.778106356	this work
-1	1.887074210 - $i$ 0.000025362	1.780524536	0.000095719	this work
		1.7805	0.0000958	[9]
-1	2.871167766 - $i$ 0.201530270	4.101494946	1.157254428	this work
-1	3.169186525 - $i$ 0.846652839	4.663461099	5.366401539	this work

TABLE II. The zeros  $k_0$  of the Jost function in the complex  $k$ -plane and the energies  $E_0$  and widths  $\Gamma$  of the  $S$ -wave bound and resonant states for the potential  $V_2(r)$ .

$\ell$	$k_0$ ( $\text{fm}^{-1}$ )	$E_0$ (MeV)	$\Gamma$ (MeV)	Ref.
0	$i$ 3.023634507	-4.571182814	0	this work
0	$i$ 1.329872758	-0.884280776	0	this work
0	2.122442334 - $i$ 0.000027859	2.252380731	0.000118256	this work
		2.25237	0.0001196	[7]
0	3.000600515 - $i$ 0.041316851	4.500948186	0.247950731	this work
		4.50	0.28	[7]
0	3.485234669 - $i$ 0.360967988	6.008281406	2.516116297	this work
0	3.974580284 - $i$ 0.788297975	7.587937367	6.266307179	this work
0	4.454733926 - $i$ 1.227097054	9.169443586	10.932781876	this work
0	4.922800349 - $i$ 1.664647328	10.731456273	16.389452891	this work
0	5.378677040 - $i$ 2.097566794	12.265190122	22.564268707	this work

TABLE III. The zeros  $k_0$  of the Jost function in the complex  $k$ -plane and the energies  $E_0$  and widths  $\Gamma$  of the bound and resonant states for the potential  $V_2(r)$  in several higher partial waves ( $1 \leq \ell \leq 4$ ).

$\ell$	$k_0$ (fm $^{-1}$ )	$E_0$ (MeV)	$\Gamma$ (MeV)
1	$i2.289054013$	-2.619884138	0
1	$1.270932606 - i0.000000043$	0.807634844	0.000000110
1	$2.674841953 - i0.002433228$	3.577386775	0.013017001
1	$3.263588553 - i0.162882441$	5.312239776	1.063162540
1	$3.742982846 - i0.564324132$	6.845729429	4.224511090
1	$4.225164261 - i0.999000737$	8.427005280	8.441884426
1	$4.696779393 - i1.437816345$	9.996210410	13.506212364
1	$5.156711217 - i1.873567558$	11.540707589	19.322893683
2	$i1.232503483$	-0.759532418	0
2	$2.183644493 - i0.000018973$	2.384151637	0.000082862
2	$3.052966547 - i0.035600651$	4.659668666	0.217375191
2	$3.527492840 - i0.341406094$	6.163323809	2.408615103
3	$1.420585762 - i0.000000016$	1.009031953	0.000000046
3	$2.760769155 - i0.001484354$	3.810922062	0.008195917
3	$3.343986231 - i0.139396664$	5.581406240	0.932281051
3	$3.802701793 - i0.526397919$	7.091723079	4.003468620
4	$2.313665822 - i0.000006013$	2.676524768	0.000027824
4	$3.170315114 - i0.023354979$	5.025176235	0.148085287
4	$3.623738918 - i0.294896551$	6.522259887	2.137256217
4	$4.076486137 - i0.706384524$	8.059380065	5.759133441

TABLE IV. Two lowest Regge trajectories for the potential  $V_2(r)$ . Only those points which correspond to the bound and resonant energies are given.

First Regge trajectory		Second Regge trajectory	
$E$ (MeV)	$\ell$	$E$ (MeV)	$\ell$
-4.571182814	0	-0.884280776	0
-2.619884138	1	0.807634844	$1.000000000 + i0.000000034$
-0.759532418	2	2.384151637	$2.000000000 + i0.000027431$
1.009031953	$3.000000000 + i0.000000013$	3.810922062	$2.999963480 + i0.003081380$
2.676524768	$4.000000000 + i0.000008632$	5.025176235	$3.990736977 + i0.065066318$

TABLE V. Third and fourth Regge trajectories for the potential  $V_2(r)$ . These trajectories start from the lowest  $S$ -wave resonances.

Third Regge trajectory		Fourth Regge trajectory	
$E$ (MeV)	$\ell$	$E$ (MeV)	$\ell$
2.252380731	$-0.000000010 + i0.000041610$	4.500948186	$-0.037200122 + i0.130360179$
3.577386775	$0.999888289 + i0.005370144$	5.312239776	$0.726629120 + i0.451038159$
4.659668666	$1.976641344 + i0.104936778$	6.163323809	$1.389037872 + i0.838973703$
5.581406240	$2.805402233 + i0.392410862$	7.091723079	$2.025517176 + i1.253031383$
6.522259887	$3.530415810 + i0.760317663$	8.059380065	$2.634772674 + i1.671995431$

# FIGURES

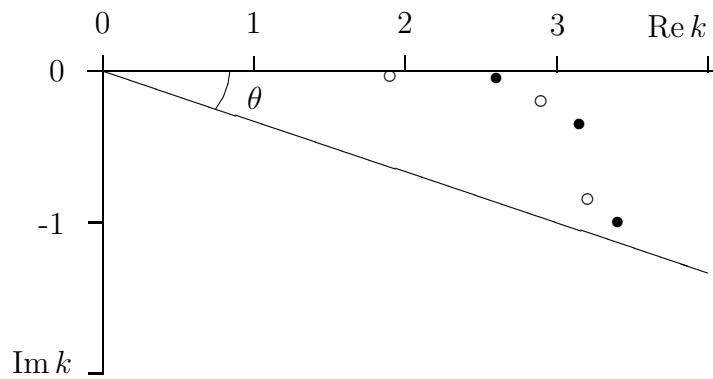


FIG. 1. The zeros of the Jost function for the  $S$ -wave resonances of the potential  $V_1(r)$  with (open circles) and without (filled circles) the Coulomb term. Exact values are given in Table I. The dividing line corresponds to the rotation angle  $\theta = 0.1\pi$ .

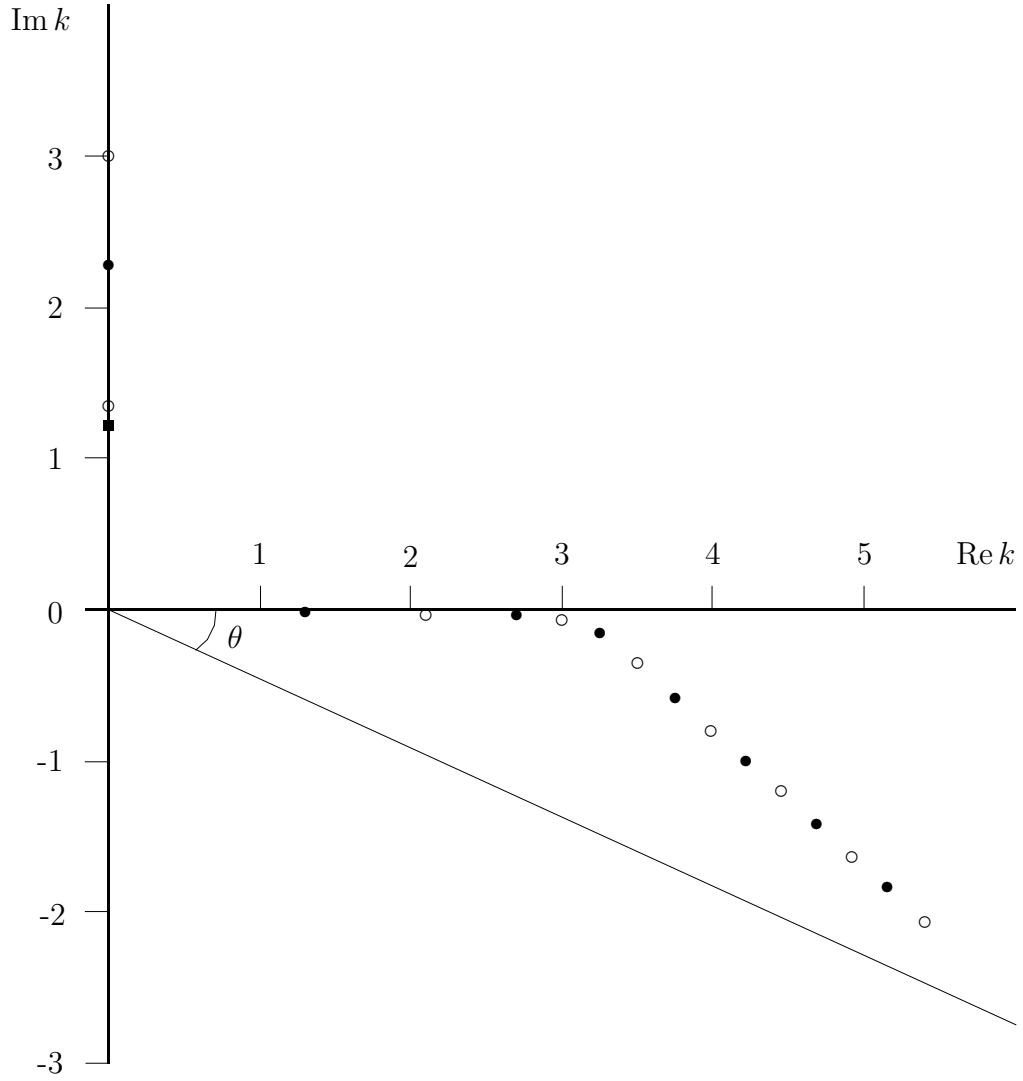


FIG. 2. The zeros of the Jost function corresponding to bound and resonant states generated by the potential  $V_2(r)$  in the  $S$ - (open circles) and  $P$ - (filled circles) partial waves. The filled box indicates the  $D$ -wave bound state. Exact values are given in Table II and III. The dividing line corresponds to the rotation angle  $\theta = 0.15\pi$ .

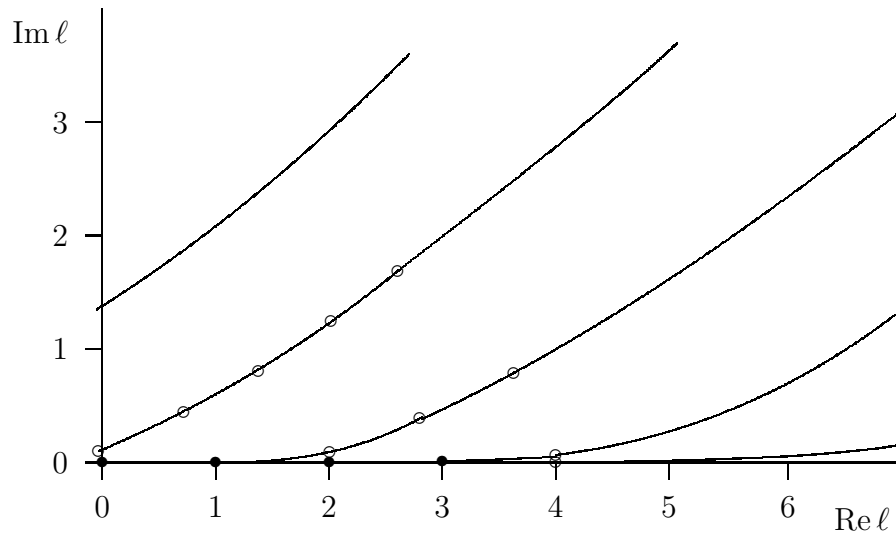


FIG. 3. The five lowest Regge trajectories for the potential  $V_2(r)$ . Exact values of the points are given in Table IV and V. Filled circles indicates points which coincide (they are at the same place of the  $\ell$ -plane but correspond to different energies) or cannot be distinguished.

## REFERENCES

- [1] Kukulin V I, Krasnopolsky V M, and Horaček J 1988 *Theory of Resonances* (Dortrecht: Kluwer Academic Publishers)
- [2] Rescigno T N and McCurdy C W 1986 *Phys. Rev. A* **34** 1882
- [3] Pupyshev V V and Rakityansky S A 1991 *Communication of JINR (Dubna)* E4-91-418
- [4] Pupyshev V V and Rakityansky S A 1994 *Z. Phys. A* **348** 227
- [5] Rakityansky S A, Sofianos S A, and Amos K 1996 *Nuovo Cim.* **111 B (3)** 363
- [6] Isaacson A D, McCurdy C W, and Miller W H 1978 *Chem. Phys.* **34** 311
- [7] C. H. Maier C H, Cederbaum L S, and Domcke W 1980 *J. Phys. B: Atom. Molec. Phys.* **13** L119
- [8] Mandelshtam V A, Ravuri T R, and Taylor H S 1993 *Phys. Rev. Lett.* **70** 1932
- [9] Yamani H A and Abdelmonem M S 1995 *J. Phys. A: Math. Gen.* **28** 2709
- [10] *Handbook of Mathematical Functions* 1964 eds. Abramowitz M and Stegun A (Washington:NBS)
- [11] Taylor J R 1972 *Scattering Theory* (New York:John Wiley & Sons, Inc.)
- [12] Mathews J and Walker R L 1964 *Mathematical Methods of Physics* (New York:W. A. Benjamin, Inc.)
- [13] The entire special issue of *Int. J. Quantum Chem.* 1978 **14**(4), is devoted to the complex-coordinate method. See also the reviews: Reinhardt W P 1982 *Ann. Rev. Phys. Chem.* **33** 223, and Ho Y K 1983 *Phys. Rep.* **99** 1
- [14] Messiah A 1970 *Quantum Mechanics* (Amsterdam:North-Holland)
- [15] Goldberger M and Watson K M 1964 *Collision Theory* (New-York:Wiley)
- [16] Sitenko A G 1991 *Scattering Theory* (Heidelberg:Springer-Verlag)
- [17] Landau L D and Lifshitz E M 1965 *Quantum Mechanics* (Oxford:Pergamon Press)
- [18] *Encyclopedic Dictionary of Mathematics* 1977 eds Iyanaga S and Kawada Y (Cambridge, Massachusetts: The MIT Press) 159
- [19] Particle Data Group 1994 *Phys. Rev. D* **50(3)** 1319
- [20] Rakityansky S A, Sofianos S A, Braun M, Belyaev V B, and W. Sandhas 1996 *Phys. Rev. C, Rapid Comm.*